A Rapid Reversed-Phase LC-MS Method for Polar Metabolite Profiling

Maxime De Neys[1,2,+], Jana K. Geuer[1,2,+], Sammy Pontrelli[1,2,]*

[+]Authors contributed equally to this work

[1]KU Leuven, Department of Biology, Lab of Microbial Metabolic Interactions, Kasteelpark Arenberg 31, B-3001 Leuven-Heverlee, Belgium

[2]VIB - KU Leuven Center for Microbiology, Lab of Microbial Metabolic Interactions, Kasteelpark Arenberg 31, B-3001 Leuven-Heverlee, Belgium

*Corresponding author

Abstract

Polar metabolites, including amino acids, nucleotides, phosphorylated metabolites, and central carbon intermediates, drive essential physiological processes but remain difficult to measure by high-throughput, reversed-phase liquid chromatography–mass spectrometry (LC-MS) due to poor retention on conventional stationary phases. Here, we establish a 3-minute injection-to-injection LC-MS method and systematically evaluate two best-in-class solid-core reversed-phase chemistries for profiling 123 biologically relevant polar metabolites, directly comparing T3-type C18 and pentafluorophenyl (PFP) stationary phases. We benchmark retention time (RT), peak shape, reproducibility, coverage, and analytical sensitivity under acidic and mildly acidic conditions. Across eight conditions, median RT coefficients of variation (CV) ranged from 1.05–1.48%, with narrow chromatographic peaks (median full width at half maximum ≈1.0 s), demonstrating stable performance under rapid gradients. The T3 column operated at pH 5 provided the highest coverage (114 of 123 metabolites) and detected 18 of 20 phosphorylated compounds, compared to 82 metabolites and 9 phosphorylated compounds under the best-performing PFP condition. Median limits of detection reached 0.02 µmol/L. Because most metabolites eluted within the first column volumes, we implemented iterative data-dependent MS/MS acquisition to improve compound annotation under short-gradient conditions, acquiring fragmentation spectra for 86 compounds in the 123 metabolite mixture without extending runtime. Performance in *Escherichia coli* intracellular extracts was robust over 480 consecutive injections,

with median RT CVs of 1.7% and consistent peak shapes. Across all evaluated metrics, the T3 stationary phase consistently outperformed PFP. Together, these results define a rapid and robust reversed-phase LC-MS workflow optimized for scalable profiling of polar and phosphorylated metabolites in high-throughput biological studies.

1 Introduction

High-throughput liquid chromatography mass spectrometry (LC-MS) analysis of highly polar metabolites remains a persistent analytical challenge, particularly for chemically and biologically important small molecules such as phosphorylated intermediates, organic acids, and nucleotides. Hydrophilic interaction chromatography (HILIC) is widely used to retain polar metabolites; however, long equilibration times, sensitivity to subtle changes in mobile phase composition and sample matrices, and retention time instability limit its suitability for high-throughput workflows[1–3]. At the other extreme, flow injection analysis (FIA) maximizes throughput by eliminating chromatographic separation entirely, but this approach exacerbates matrix effects, limits analyte discrimination, and reduces confidence in metabolite annotation[4]. Recent fast metabolomics methods using mixed-mode LC or HILIC coupled to ion mobility have demonstrated that short (≈3.5-5 min) gradients can still provide broad metabolome coverage, but typically at the cost of specialized hardware that is not universally available (i.e., quaternary or tertiary pumps or ion mobility-enabled mass spectrometers)[5,6]. Consequently, there remains a need for LC-MS methods that occupy a middle ground, offering short method times while retaining sufficient chromatographic structure to support robust metabolite profiling and annotation on standard ultra-high performance liquid chromatography (UHPLC) systems.

Conventional C18 stationary phases provide limited retention for highly polar compounds; however, recent advances in reversed-phase stationary phase design have expanded the applicability of RP-LC to more polar analytes. Functionalized chemistries such as pentafluorophenyl (PFP) phases, which provide mixed-mode interactions for retaining diverse polar metabolites[7], and polar-compatible C18 T3-type phases, which maintain full wettability and therefore stable retention in 100% aqueous mobile phases, enable robust retention of polar compounds[8]. Both column types have been shown to extend reversed-phase retention while preserving short equilibration times[3,8]. In parallel, the adoption of solid-core particles and reduced particle sizes has enabled higher separation efficiency and shorter gradients without prohibitive backpressure[9]. Despite these developments, the performance limits of such approaches under extreme throughput constraints, particularly for highly polar and phosphorylated metabolites, have not been systematically evaluated.

Here, we systematically evaluate two complementary solid-core reversed-phase columns, a PFP phase and a T3-type C18 (T3) phase, across acidic and mildly acidic mobile phase conditions to assess their suitability for fast LC-MS analysis of highly polar metabolites. To develop a 3-minute

sample-to-sample injection method, we benchmark retention time stability, peak shape, reproducibility, and analytical sensitivity for a panel of 123 polar metabolites spanning amino acids, organic acids, nucleotides, and phosphorylated intermediates.

Tandem mass spectrometry (MS/MS) provides structurally informative fragmentation spectra that are useful for the identification of metabolites. Although the highest annotation confidence is achieved through direct comparison with analytical standards, matching experimental spectra to reference libraries can substantially aid in the annotation of unknown compounds[10]. A widely used mode to collect such fragmentation spectra is data-dependent acquisition (DDA). Precursor ions with the highest intensities in MS1 are selected. During subsequent fragmentation, only the fragments of these targeted ions are recorded. With proper optimisation, annotation of unknown metabolites can be improved with DDA[11].

Under ultra-fast chromatographic conditions, retention of highly polar metabolites is limited and chromatographic peaks are narrow, constraining the time available for tandem mass spectrometry (MS/MS) acquisition. In conventional data-dependent acquisition (DDA), the most intense precursor ions detected in MS1 are selected for fragmentation within a single injection; however, short peak widths restrict the number of precursors that can be sampled, limiting MS/MS coverage and annotation depth. To overcome this limitation while preserving a 3-minute runtime, we implemented iterative DDA with dynamic exclusion[12]. In this approach, the same sample is analyzed repeatedly, and precursor ions fragmented in earlier injections are excluded from subsequent runs, enabling progressive acquisition of MS/MS spectra from lower-abundance ions. This strategy increases cumulative MS/MS coverage across injections without extending chromatographic cycle time, providing complementary structural information to strengthen metabolite annotation under ultra-fast separation conditions.

Central carbon metabolites are used as a chemically demanding test set, as they encompass a broad range of highly polar analytes that challenge both chromatographic retention and ionization efficiency. Together, this work addresses practical design considerations for high-throughput reversed-phase LC-MS analysis of polar metabolites, providing an analytically-based middle ground to both HILIC- and FIA-based workflows when speed, robustness, and annotation confidence must be balanced.

2 Experimental Section

2.1. Metabolite standards

97 All 123 standards were purchased from Sigma-Aldrich, weighed, and dissolved in a final
98 concentration of 20 mmol/L per stock solution. From these stock solutions, a standard mix of 50
99 µmol/L per metabolite was created and stored in aliquots at -80°C.

100 **2.2 LC-MS conditions**

101 LC-MS measurements were performed using an Agilent Infinity III stack either with an Agilent
102 InfinityLab Poroshell 120 PFP column (2.1 mm x 50 mm, 1.9 µm) operated in reversed phase,
103 with an InfinityLab Poroshell 120 PFP guard column (2.1 mm x 5 mm, 1.9 µm) at 30°C, or with a
104 Waters CORTECS™ Premier T3 VanGuard™ FIT column (2.1 mm x 50 mm, 1.6 µm) operated in
105 revered phase at 50°C. The autosampler was kept at 4°C and the injection volume was 5 µL. The
106 injector needle was washed before each injection consecutively with three solutions for 3 s each
107 to prevent carry-over: Methanol (MeOH, Fisher Scientific, USA)/H_2O 50/50 (v/v), 2-Propanol (IPA,
108 Biosolve, the Netherlands)/H_2O (Milli-Q IQ 7000 purification system (MilliporeSigma, USA) 50/50
109 (v/v), and eluent A. Gradient elution was carried out at 1 mL/min with eluent A consisting of
110 H_2O/Acetonitrile (ACN, Fisher Scientific, USA) 100/0 (v/v) and eluent B consisting of ACN/H_2O
111 90/10 (v/v), both containing either 0.1% formic acid (TCI Chemicals, Japan) (pH 3) or 0.1%
112 ammonium acetate (Sigma-Aldrich, USA) buffer set to pH 5 using acetic acid (TCI Chemicals,
113 Japan). After evaluating different higher organic compositions (70-80% B), the final gradient was
114 as follows: 0 – 0.5 min 0% B, 0.5 – 0.9 min increased to 10% B, 0.9 – 1.5 min increased to 80%
115 B, 1.5 – 1.98 min held at 80% B, 1.98 – 1.99 min returned to 0% B, and held for 1 min for re-
116 equilibration. An Agilent Revident LC/Q-TOF was used for measurements, operated both in
117 negative and in positive ionization modes with an m/z range of 20 – 1700 in 750 V stable mode.
118 Source conditions were set to a gas temperature of 325 °C, drying gas of 10 L/min, nebulizer
119 pressure of 30 psi, sheath gas temperature of 250 °C, and sheath gas flow of 11 L/min. The
120 capillary voltage was set to 3500 V, with a nozzle voltage of 1000 V and octopole RF of 750 V.
121 The capillary current was 0.24 µA and the chamber current (CA) was 1.7 µA. The fragmentor
122 voltage was set to 110 V and the skimmer to 45 V.

123 **2.3 Iterative MS/MS**

124 Iterative MS/MS experiments were performed on the pre-mixed standard mixture. The standard
125 was thawed and diluted to a final concentration of 25 µmol/L. LC conditions were as described
126 under LC-MS conditions exclusively on the T3 column. DDA was conducted on an Agilent
127 Revident QTOF operated in both positive and negative electrospray ionization modes with source
128 conditions as described under LC-MS conditions. A maximum of four precursors per cycle was

129 selected using a narrow 1.3 m/z isolation window. An absolute intensity threshold of 5000 counts
130 and a relative threshold of 0.03 % were applied for precursor selection. Charge state preference
131 was restricted to singly charged ions and ions of unknown charge. Iterative MS/MS precursor
132 exclusion was performed with a mass tolerance of ±20 ppm and a retention time exclusion window
133 of ±0.5 min. Active exclusion was enabled after one MS/MS spectrum and released after 0.2 min.
134 For MS only acquisition, data were acquired at 10 spectra/s with an acquisition time of 100 ms
135 per spectrum. For MS/MS acquisition, a rate of 5 spectra/s was used with 200 ms per spectrum
136 with the collision energy set to 20 eV.

137 **2.4 Data analysis**

138 Data analysis were performed using Agilent MassHunter Qualitative/Quantitative Analysis
139 software and R 4.5.1/R Studio 2025.09.2+418 with the packages tidyr[13], dplyr[14], and ggplot2[15].
140 MassHunter software was used to integrate peaks (Agile2 Integrator), fit polynomial calibration
141 curves, and calculate retention times, full width at half maximum (FWHM), and signal-to-noise
142 (S/N) ratios. Standards were measured for the following concentrations: 50, 25, 12.5, 10, 6.25,
143 3.125, 1.565, 0.781, 0.391, 0.195, 0.098, 0.049, and 0.024 µmol/L. Mean retention times (RT)
144 were calculated using 20 replicate injections at 10 µmol/L. For the determination of the limit of
145 detection (LOD) and limit of quantification (LOQ), 4 replicate injections were acquired at each
146 concentration level, and levels with at least 3 successful replicate injections were retained. For
147 each eligible level, the mean S/N ratio was calculated from the 3-4 replicates, and the LOD and
148 LOQ were assigned as the lowest concentrations with mean S/N ≥ 3 and ≥ 10, respectively.
149 Coefficient of variations, limit of detection, limit of quantification, and retention factors were
150 computed in R. Retention factors (R_f) were defined as the difference between standards' mean
151 retention times ($\bar{t}_R$) and the void time (t_0), divided by the void time.

152 $$R_f = \frac{(\bar{t}_R - t_0)}{t_0}$$

153 For iterative MS data files were processed using MSConvert (ProteoWizard)[16] , using the Peak
154 Picking filter with vendor algorithm for MS1-2. Afterwards, the data and spectral libraries were
155 imported into MZmine4[17] and processed using a structured batch workflow. Mass detection was
156 performed with noise levels of 500 (MS^1) and 200 (MS/MS). MS^n tree building used an m/z
157 tolerance of 20 ppm. Isotope detection (H,C,N,O,S) was applied with 20 ppm and maximum
158 charge 1, selecting the most intense isotope. Features were aligned using the Join Aligner
159 (15 ppm, 0.03 min RT tolerance, equal weighting). Correlation grouping used an RT tolerance of

160 0.03 min, minimum feature height 100 000, and an intensity threshold of 100. Ion identity
161 networking was performed with 10 ppm intra-sample m/z tolerance, using an adduct library
162 containing $[M–H]^-$, $[M+H]^+$, $[M+Na]^+$, and $[M+NH_4]^+$. MS/MS spectral matching was performed
163 using the publicly available libraries MassBank[18], MassBank of North America (MoNA[19]), and
164 GNPS[20] in MZmine on merged representative MS/MS scans (per energy and merged across
165 energies). Matching used 10 ppm tolerance for merging, 8 ppm for precursors, and 10 ppm for
166 fragments. Precursor ions were removed prior to scoring. A minimum of 2 matched fragment ions
167 and weighted cosine similarity with a minimum cosine score of 0.65 were required. After export,
168 the annotations were matched against the list of standards was performed in R4.5.2/R studio
169 2025.09.2+418 using the data.table package[21].

170 **2.5 Bacterial growth conditions and extraction of metabolites**

171 *Escherichia coli* BW25113 was stored at -80°C in glycerol stocks and streaked onto Luria-Bertani
172 (LB) plates containing 2% (w/v) agar. A single colony was inoculated into 3 mL of liquid LB and
173 grown overnight at 37°C with shaking at 200 rpm. The overnight culture was diluted 1:100 into
174 fresh LB and incubated at 37°C, 200 rpm until mid-exponential phase ($OD_{600} \approx 0.5$). Cells were
175 harvested by centrifugation with subsequent removal of the supernatant. For intracellular
176 metabolite extraction, the pellet was resuspended in cold extraction solvent consisting of
177 ACN/MeOH/H_2O, 40:40:20 (v/v/v) and incubated for one hour at -20°C. Intracellular metabolite
178 extracts were separated by centrifugation, and the supernatant was collected and filtered through
179 a 0.2 µm membrane prior to LC-MS analysis.

180 # 3 Results

181 **3.1 Chromatographic performance under 3-minute gradients**

182 To determine whether ultra-fast reversed-phase separations can provide sufficient
183 chromatographic structure for polar metabolites, we first evaluated chromatographic performance
184 under a 3-minute injection-to-injection workflow using two solid-core reversed-phase stationary
185 phases (PFP and T3) operated at pH 3 and pH 5 **(Figure 1)**. Both columns provided a reproducible
186 TIC **(Figure S1)** at a flow rate of 1 mL min^{-1} without exceeding instrument backpressure limits.
187 The Premier T3 column exhibited a more rapid increase in backpressure over time (0.05
188 bar/injection) relative to the Poroshell PFP column (0.01 bar/injection), consistent with its smaller
189 particle size and inlet frit.

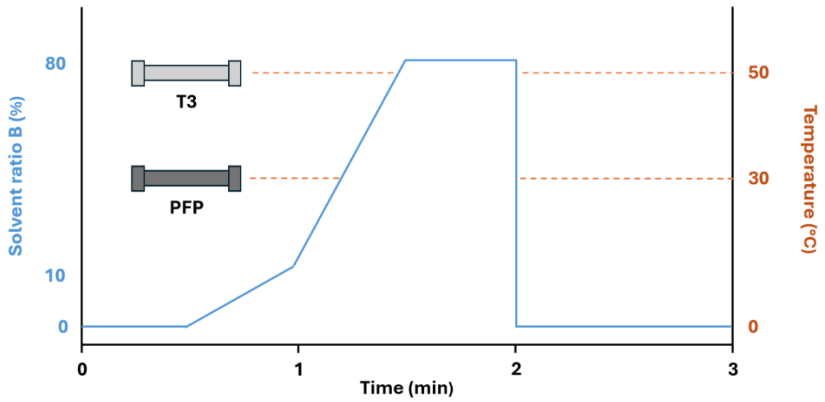

Figure 1. Reversed-phase gradient program (Percentage of mobile phase B over time, blue) and column temperature configurations for the different columns, which were used for the 3-min LC-MS method (orange).

Across all conditions, detected metabolites exhibited modest but reproducible retention, eluting with median RT of 1.7 column volumes across all compounds in any condition **(Table S1)**. Despite the short gradient, retention time precision was high with median RT CVs ranging from 1.05-1.48% across all column, pH, and ionization mode combinations. Chromatographic peaks remained narrow and well defined, with a median FWHM at 1.038 s. Together, these results demonstrate that even under extreme 3-minute gradient conditions, reversed-phase LC provides stable and reproducible analysis.

3.2 Effect of column chemistry and pH on polar metabolite coverage

To assess how column chemistry and mobile phase pH influence analytical coverage, we quantified the number of detected metabolites across all column, pH, and ionization mode combinations using a panel of 123 highly polar compounds. Across conditions, the number of detected metabolites ranged from 69 to 114, indicating a strong dependence of coverage on both stationary phase and mobile phase composition **(Table S1, Figure 2A).** Negative ion mode consistently yielded higher coverage than positive mode. In negative mode, the T3 column outperformed the PFP column at both pH values, with the highest overall coverage observed for T3 operated at pH 5 (114 detected metabolites). In contrast, the best-performing PFP condition detected 82 metabolites. In negative ion mode, metabolites were consistently detected as deprotonated species across all column and pH conditions. In positive mode, most compounds were observed as protonated species, although several highly oxygenated metabolites, predominantly carbohydrates and polyols, were detected preferentially or exclusively as sodium adducts (**Table S2**). Across all conditions, four metabolites (phenyl acetate, ethyl-3-methyl-2-oxobutyrate, guanosine 5'-triphosphate, and 2,3-diphospho-D-glucuronic acid) were not detected,

likely reflecting inherently poor ionization efficiency, instability or adsorption-related losses. To further contextualize differences in metabolite coverage, analytical sensitivity was assessed by estimating LOD and LOQ for the standard mixture under each condition. Across compounds, median LODs were comparable between the T3 and PFP columns at pH 3 (0.0244 µmol/L in negative mode for both), but were lower for T3 at pH 5 (0.0977 µmol/L compared to 0.1953 µmol/L for PFP). LOQ trends followed a similar pattern, with T3 operated at pH 3 yielding the lowest values overall (0.0244 µmol/L) (**Table S3**).

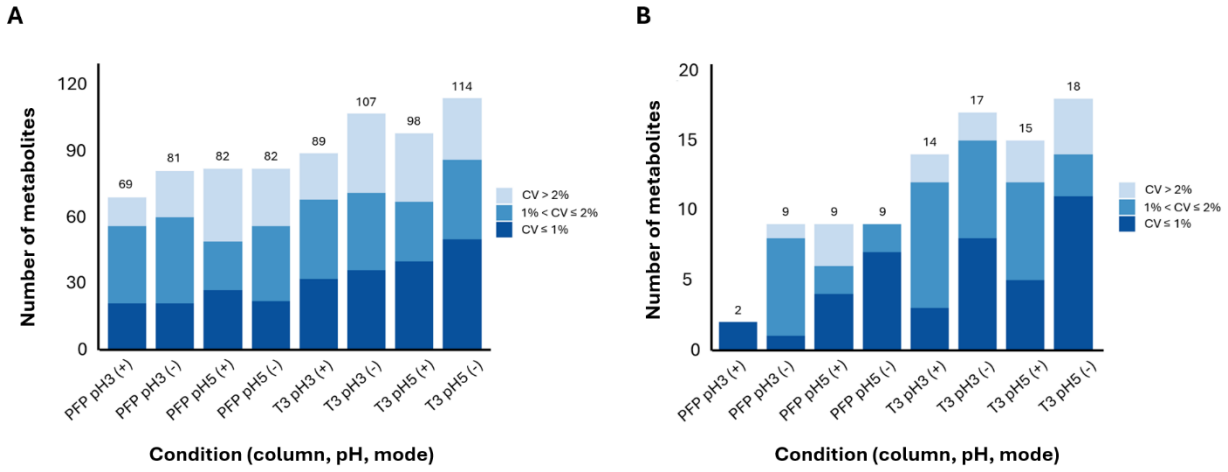

Figure 2. Effect of column chemistry, mobile phase pH, and ionization mode on metabolite coverage under 3-min gradient conditions. The number of detected metabolites across PFP and T3 columns operated at pH 3 and pH 5 in positive and negative ionization modes is shown for (A) the full polar metabolite panel (n = 123) and (B) the phosphorylated subset (n = 20).

Differences between stationary phases were most pronounced for phosphorylated compounds. Of the 20 phosphorylated metabolites included in the standard panel, 9 were detected under at least one PFP condition, whereas 18 were detected in at least on T3 condition **(Figure 2B)**. This improved coverage is likely due to the bio-inert T3 hardware, which reduces analyte-metal interactions that disproportionately affect phosphate-containing metabolites.

Mobile phase pH further modulated coverage, with pH 5 conditions generally enabling detection of a broader range of polar metabolites than pH 3 **(Figure 2)**. This effect was most evident for phosphorylated compounds, which showed improved signal intensity and peak shape under mildly acidic conditions. For example, Adenosine 5'-triphosphate exhibited a substantially sharper, more symmetric peak and increased signal intensity at pH 5 compared to pH 3 on the T3 column **(Figure 3)**. Similar trends were observed for other phosphorylated intermediates **(Table S4)**. Retention time reproducibility followed similar trends. For the T3 column operated at pH 5 in

239 negative mode, 50 metabolites exhibited RT CVs ≤1% and 86 exhibited RT CVs ≤2%, compared
240 to 22 and 56, respectively, for the best-performing PFP condition. Our results, taken together,
241 identify the Premier T3 column operated at pH 5 as the most effective condition for maximizing
242 coverage of highly polar, and in particular phosphorylated metabolites.

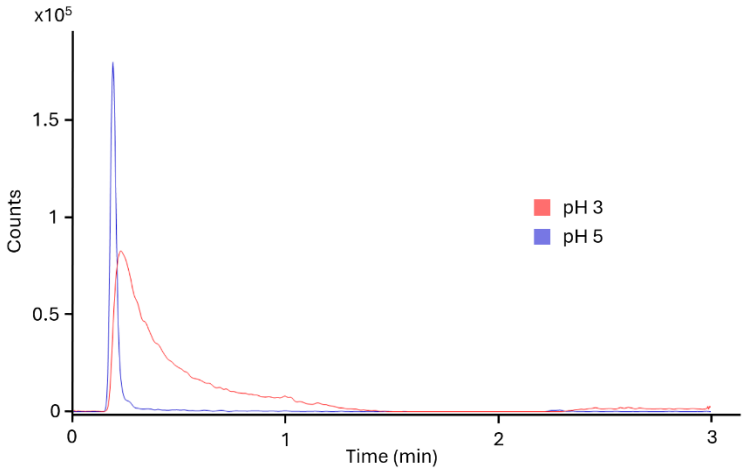

243

244 **Figure 3. Effect of mobile phase pH on extracted ion chromatograms of adenosine 5′-triphosphate.** Smoothed
245 extracted ion chromatograms (EICs) of adenosine 5'-triphosphate (50 µmol/L) acquired in negative ionization mode
246 using T3 are shown for pH3 (pink) and pH5 (violet).

247 **3.3 Iterative MS/MS improves metabolite annotation despite limited retention**

248 Despite the broad metabolite coverage achieved under this high-throughput workflow, the
249 shortened gradient inherently limits chromatographic separation, constraining confident
250 annotation of early, co-eluting compounds. To improve annotation confidence without
251 compromising throughput, we employed repeated injections of a standard mixture to
252 progressively acquire MS/MS spectra. Rather than relying on comprehensive MS/MS coverage
253 within a single injection, this multi-injection strategy enables accumulation of fragmentation
254 spectra for a larger fraction of features. In practice, this strategy allows MS/MS information to be
255 accumulated from pooled samples, with consistent retention times and peak shapes used to
256 support metabolite annotation across large sample sets analyzed under identical conditions.

257 Using this approach, we annotated MS/MS spectra for 86 of the 123 metabolites through spectral
258 library matching in MZmine 4. At pH 3, we annotated 72 metabolites in total. Of these, 24 were
259 detected in both ionization modes, 21 were annotated exclusively in negative mode, and 27 were
260 annotated exclusively in positive mode. At pH5, of the 69 annotated metabolites 27 were picked
261 up at both polarities, 22 in negative and 20 in positive mode only **(Figure 4A)**. Samples were
262 iterated ten times. For all tested conditions most metabolites were annotated in the first and

second iteration. Additional MS/MS spectra were, however, acquired up to the last acquisition in pH3, positive mode **(Figure 4B)**.

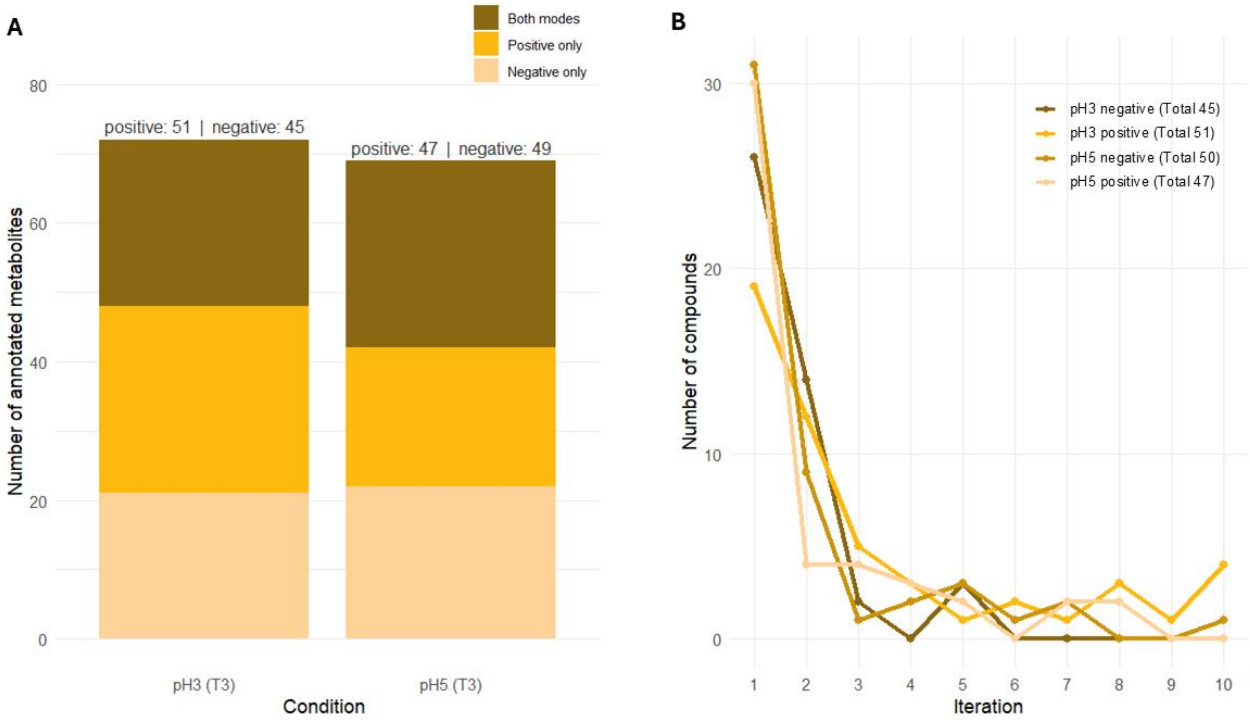

Figure 4. Annotations by iterative MS/MS. A: metabolites annotated based on spectral library matching by pH. In total, 69 metabolites were annotated at pH 5 and 72 at pH3 on a T3 column. Dark orange: compounds were annotated in both positive and negative mode. orange: compounds were only annotated in positive mode, bright orange: compounds were only annotated in negative mode. B: annotated compounds by number of iteration. Brown: Annotations at pH3, negative mode, dark orange: annotations at pH5, negative mode, orange: annotations at pH3 positive mode, light orange: annotations at pH5, positive mode.

Annotation success was highest for metabolites detected with stable retention times and sufficient precursor intensity across injections, while low-abundance compounds and those exhibiting poor ionization remained challenging. We further confirm that repeated injections can be used to progressively acquire MS/MS spectra substantially, with the first iteration only picking up between 35 and 65% of the total annotated compounds.

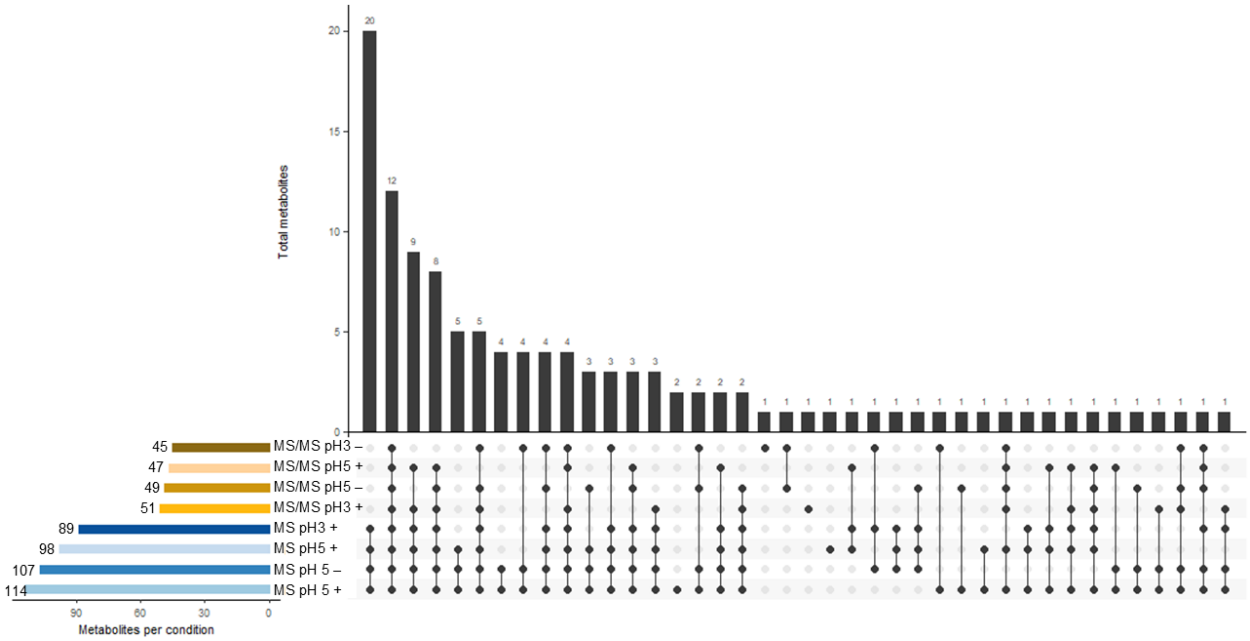

Figure 5: UpSet plot visualising the intersecting sets of metabolites found by condition on a T3 column. Bars on the left show numbers of metabolites detected per condition. Blue: MS detection. Orange: iterative MS/MS annotated compounds. Grey bars on top show the number of metabolites identified for a specific set of conditions. The largest set of metabolites was found in all MS modes, the second largest overlap (12) was found between all conditions

In total, a set of 12 metabolites overlapped in all acquisition modes tested on the T3 column (standards measured in MS1 and using iterative MS/MS). Only 3 Metabolites in total were exclusively picked up by iterative MS/MS measurements. The largest overlap (20 metabolites) was found between all MS1 conditions **(Figure 5)**. Overall, this overlap confirms that the detection of metabolites is highly reproducible across modes. Iterative MS/MS enhanced the spectral completeness, consistent with the observation that repeated injections substantially increasing MS/MS annotation rates, compensating for spectra missed in initial runs, particularly when co-eluting or structurally similar precursors compete within the ddA selection window, leading to under sampling of lower-intensity ions. Overall, these results demonstrate that combining stable MS1 acquisition with iterative MS/MS provides a more complete and reliable structural dataset, consistent with earlier reports on improved annotation yields through enhanced fragmentation strategies.

3.4 Method robustness and annotation performance in a complex biological matrix

To evaluate method robustness and annotation performance in a realistic sample matrix, we analyzed an *E. coli* intracellular extract using the optimized T3 column operated at pH 5 in negative ionization mode. The extract was injected repeatedly over 480 consecutive injections

298 under identical chromatographic conditions to assess retention time stability and peak shape
299 reproducibility over extended use.

300 Across the injection series, 94 out of the 123 monitored metabolites were detected in more than
301 95% of injections (12 of 20 phosphorylated metabolites), indicating robust detection in complex
302 *E. coli* matrix (**Table S5**). Median RT CVs across detected features were 1.7%, with 21
303 metabolites exhibiting RT CVs ≤1% and 51 metabolites exhibiting RT CVs ≤2% over the full
304 injection sequence. Retention times in matrix closely matched those of neat standards, with a
305 median ΔRT of 0.168 s across 94 metabolites. Peak shapes remained consistent throughout the
306 run, with a median FWHM of 0.95 s across detected metabolites and no systematic broadening
307 or tailing observed, indicating stable chromatographic performance under prolonged high-
308 throughput operation. Backpressure increased gradually over the injection series but remained
309 within acceptable operating limits, consistent with expectations for extended use of short, small-
310 particle columns. Together, these results demonstrate that the 3-minute reversed-phase LC-MS
311 method maintains retention time stability, peak integrity, and metabolite detectability in complex
312 biological matrices over extended high-throughput operation, supporting its suitability for large-
313 scale metabolomic studies.

314 4 Discussion

315 In this study, we developed and systematically evaluated a rapid reversed-phase LC-MS method
316 for high-throughput analysis of highly polar metabolites using solid-core stationary phases under
317 short-gradient conditions. PFP could resolve many compounds and has been shown effective for
318 quantitative metabolomics in bacteria by giving good retention, sensitivity and reproducibility[22].
319 Among the tested configurations, however, the T3-type C18 stationary phase operated at pH 5
320 provided the most effective balance of metabolite coverage, retention time reproducibility, and
321 peak quality for polar and phosphorylated metabolites, with bio-inert hardware further reducing
322 analyte-metal interactions and the associated losses particularly affecting phosphate-containing
323 metabolites[23,24].

324 Despite limited retention under these extreme throughput constraints, the method delivers stable,
325 narrow peaks suitable for extended injection series, while progressive MS/MS acquisition
326 improves annotation without sacrificing speed. This effect is consistent with previous findings,
327 showing that iterative MS/MS increases annotation yields in comparison to regular DDA,
328 especially when structurally similar compounds are co-eluting[25]. While this strategy improves
329 annotation confidence under short-gradient conditions, co-elution of matrix components is

unavoidable, and ion suppression effects cannot be fully eliminated[26]. Accordingly, the method is intended for high-throughput metabolite profiling rather than absolute quantification, deliberately prioritizing analytical speed and robustness over maximal chromatographic resolution.

Alternative strategies for rapid metabolome coverage have combined zwitterionic HILIC with ion-mobility separation[27] or employed mixed-mode stationary phases with ternary gradients[28] to achieve 3.5-5 min separations and broad metabolome coverage. While effective, these approaches require specialized hardware, including ion-mobility mass spectrometers or non-standard LC pump configurations (i.e., ternary or quaternary systems), which can limit routine adoption. By comparison, the approach presented here profiles highly polar and phosphorylated metabolites using a T3 reversed-phase column operated with a simple binary gradient on conventional LC-MS instrumentation, supporting accessibility and ease of deployment across laboratories.

Together, this work addresses practical design considerations for fast reversed-phase LC-MS analysis of polar metabolites and establish a framework for balancing throughput, robustness, and annotation confidence. Importantly, the method described here deliberately focuses on the early portion of the reversed-phase gradient, where highly polar metabolites elute. In real biological samples, less polar and nonpolar metabolites would be expected to elute later in the gradient and were not evaluated in the present study. As such, this method provides a flexible and analytically grounded option for studies that require rapid, scalable metabolite profiling.

References

(1) Cai, X.; Zou, L.; Dong, J.; Zhao, L.; Wang, Y.; Xu, Q.; Xue, X.; Zhang, X.; Liang, X. Analysis of Highly Polar Metabolites in Human Plasma by Ultra-Performance Hydrophilic Interaction Liquid Chromatography Coupled with Quadrupole-Time of Flight Mass Spectrometry. *Analytica Chimica Acta* **2009**, *650* (1), 10–15. https://doi.org/10.1016/j.aca.2009.01.054.

(2) Langová, A.; Manzi, M.; Brejchová, J.; Kuda, O.; Holčapek, M.; Jirásko, R. Enhancing Metabolite Coverage Using Dedicated Mobile Phases for Individual Polarity Modes in HILIC-MS. *Anal Bioanal Chem* **2026**, *418* (2), 747–757. https://doi.org/10.1007/s00216-025-06189-0.

(3) Sato, M.; Ikeda, K. Untargeted Analysis of Hydrophilic Metabolites Using Enhanced LC-MS Separation with a Pentafluoro Phenylpropyl-Functionalized Column and Prediction-Based MS/MS Spectrum Annotation. *Metabolomics* **2025**, *21* (4), 79. https://doi.org/10.1007/s11306-025-02272-w.

(4) Farke, N.; Schramm, T.; Verhülsdonk, A.; Rapp, J.; Link, H. Systematic Analysis of In-Source Modifications of Primary Metabolites during Flow-Injection Time-of-Flight Mass Spectrometry. *Analytical Biochemistry* **2023**, *664*, 115036. https://doi.org/10.1016/j.ab.2023.115036.

(5) Imado, Y.; Takahashi, M.; Soma, Y.; Aburaya, S.; Nakatani, K.; Hanai, T.; Bamba, T.; Izumi, Y. Evaluation of LC/MS Methods for Hydrophilic Metabolites to Enable Integration of Human Blood Metabolome Data. *Mass Spectrometry* **2026**, *15* (1), A0188–A0188. https://doi.org/10.5702/massspectrometry.A0188.

(6) Nacham, O.; Brown, J. W.; Maneshi, M. M.; Kurschner, V.; Sheehan, M.; Sadowski, R.; Ling, C.; Talaty, N.; Johnson, R.; Swensen, A. M. A Mixed-Mode LC-MS-Based Method for Comprehensive Analysis of NAD and Related Metabolites from Biological Sample Matrices. *Sci Rep* **2025**, *15* (1), 14187. https://doi.org/10.1038/s41598-025-97834-2.

(7) Takenaka, M.; Yoshida, T.; Hori, Y.; Bamba, T.; Mochizuki, M.; Vavricka, C. J.; Hattori, T.; Hayakawa, Y.; Hasunuma, T.; Kondo, A. An Ion-Pair Free LC-MS/MS Method for Quantitative Metabolite Profiling of Microbial Bioproduction Systems. *Talanta* **2021**, *222*, 121625. https://doi.org/10.1016/j.talanta.2020.121625.

(8) Cheng, X.-D.; Zhang, Z.; Li, Y.-P.; Dai, X. Design and Evaluation of C18 Stationary Phases with Different Polar-Embedded Groups for Liquid Chromatography. *Analytica Chimica Acta* **2025**, *1338*, 343585. https://doi.org/10.1016/j.aca.2024.343585.

(9) Perchepied, S.; Ritchie, H.; Desmet, G.; Eeltink, S. Insights in Column Packing Processes of Narrow Bore and Capillary-Scale Columns: Methodologies, Driving Forces, and Separation Performance – A Tutorial Review. *Analytica Chimica Acta* **2022**, *1235*, 340563. https://doi.org/10.1016/j.aca.2022.340563.

(10) Godzien, J.; Gil De La Fuente, A.; Otero, A.; Barbas, C. Metabolite Annotation and Identification. In *Comprehensive Analytical Chemistry*; Elsevier, 2018; Vol. 82, pp 415–445. https://doi.org/10.1016/bs.coac.2018.07.004.

(11) Defossez, E.; Bourquin, J.; Von Reuss, S.; Rasmann, S.; Glauser, G. Eight Key Rules for Successful Data-dependent Acquisition in Mass Spectrometry-based Metabolomics. *Mass Spectrometry Reviews* **2023**, *42* (1), 131–143. https://doi.org/10.1002/mas.21715.

(12) Yu, M.; Dolios, G.; Petrick, L. Reproducible Untargeted Metabolomics Workflow for Exhaustive MS2 Data Acquisition of MS1 Features. *J Cheminform* **2022**, *14* (1), 6. https://doi.org/10.1186/s13321-022-00586-8.

(13) Wickham, H.; Vaughan, D.; Girlich, M. Tidyr: Tidy Messy Data, 2014, 1.3.2. https://doi.org/10.32614/CRAN.package.tidyr.

(14) Wickham, H.; François, R.; Henry, L.; Müller, K.; Vaughan, D. Dplyr: A Grammar of Data Manipulation, 2014, 1.2.0. https://doi.org/10.32614/CRAN.package.dplyr.

(15) Wickham, H. *Ggplot2: Elegant Graphics for Data Analysis*, Second edition.; Use R!; Springer international publishing: Cham, 2016.
(16) Adusumilli, R.; Mallick, P. Data Conversion with ProteoWizard msConvert. In *Proteomics*; Comai, L., Katz, J. E., Mallick, P., Eds.; Methods in Molecular Biology; Springer New York: New York, NY, 2017; Vol. 1550, pp 339–368. https://doi.org/10.1007/978-1-4939-6747-6_23.
(17) Schmid, R.; Heuckeroth, S.; Korf, A.; Smirnov, A.; Myers, O.; Dyrlund, T. S.; Bushuiev, R.; Murray, K. J.; Hoffmann, N.; Lu, M.; Sarvepalli, A.; Zhang, Z.; Fleischauer, M.; Dührkop, K.; Wesner, M.; Hoogstra, S. J.; Rudt, E.; Mokshyna, O.; Brungs, C.; Ponomarov, K.; Mutabdžija, L.; Damiani, T.; Pudney, C. J.; Earll, M.; Helmer, P. O.; Fallon, T. R.; Schulze, T.; Rivas-Ubach, A.; Bilbao, A.; Richter, H.; Nothias, L.-F.; Wang, M.; Orešič, M.; Weng, J.-K.; Böcker, S.; Jeibmann, A.; Hayen, H.; Karst, U.; Dorrestein, P. C.; Petras, D.; Du, X.; Pluskal, T. Integrative Analysis of Multimodal Mass Spectrometry Data in MZmine 3. *Nat Biotechnol* **2023**, *41* (4), 447–449. https://doi.org/10.1038/s41587-023-01690-2.
(18) MassBank consortium and its contributors. MassBank/MassBank-Data: Release Version 2025.05.1, 2025. https://doi.org/10.5281/ZENODO.15341877.
(19) MassBank of North America (MoNA). https://mona.fiehnlab.ucdavis.edu (accessed 2026-10-31).
(20) Wang, M.; Carver, J. J.; Phelan, V. V.; Sanchez, L. M.; Garg, N.; Peng, Y.; Nguyen, D. D.; Watrous, J.; Kapono, C. A.; Luzzatto-Knaan, T.; Porto, C.; Bouslimani, A.; Melnik, A. V.; Meehan, M. J.; Liu, W.-T.; Crüsemann, M.; Boudreau, P. D.; Esquenazi, E.; Sandoval-Calderón, M.; Kersten, R. D.; Pace, L. A.; Quinn, R. A.; Duncan, K. R.; Hsu, C.-C.; Floros, D. J.; Gavilan, R. G.; Kleigrewe, K.; Northen, T.; Dutton, R. J.; Parrot, D.; Carlson, E. E.; Aigle, B.; Michelsen, C. F.; Jelsbak, L.; Sohlenkamp, C.; Pevzner, P.; Edlund, A.; McLean, J.; Piel, J.; Murphy, B. T.; Gerwick, L.; Liaw, C.-C.; Yang, Y.-L.; Humpf, H.-U.; Maansson, M.; Keyzers, R. A.; Sims, A. C.; Johnson, A. R.; Sidebottom, A. M.; Sedio, B. E.; Klitgaard, A.; Larson, C. B.; Boya P, C. A.; Torres-Mendoza, D.; Gonzalez, D. J.; Silva, D. B.; Marques, L. M.; Demarque, D. P.; Pociute, E.; O'Neill, E. C.; Briand, E.; Helfrich, E. J. N.; Granatosky, E. A.; Glukhov, E.; Ryffel, F.; Houson, H.; Mohimani, H.; Kharbush, J. J.; Zeng, Y.; Vorholt, J. A.; Kurita, K. L.; Charusanti, P.; McPhail, K. L.; Nielsen, K. F.; Vuong, L.; Elfeki, M.; Traxler, M. F.; Engene, N.; Koyama, N.; Vining, O. B.; Baric, R.; Silva, R. R.; Mascuch, S. J.; Tomasi, S.; Jenkins, S.; Macherla, V.; Hoffman, T.; Agarwal, V.; Williams, P. G.; Dai, J.; Neupane, R.; Gurr, J.; Rodríguez, A. M. C.; Lamsa, A.; Zhang, C.; Dorrestein, K.; Duggan, B. M.; Almaliti, J.; Allard, P.-M.; Phapale, P.; Nothias, L.-F.; Alexandrov, T.; Litaudon, M.; Wolfender, J.-L.; Kyle, J. E.; Metz, T. O.; Peryea, T.; Nguyen, D.-T.; VanLeer, D.; Shinn, P.; Jadhav, A.; Müller, R.; Waters, K. M.; Shi, W.; Liu, X.; Zhang, L.; Knight, R.; Jensen, P. R.; Palsson, B. Ø.; Pogliano, K.; Linington, R. G.; Gutiérrez, M.; Lopes, N. P.; Gerwick, W. H.; Moore, B. S.; Dorrestein, P. C.; Bandeira, N. Sharing and Community Curation of Mass Spectrometry Data with Global Natural Products Social Molecular Networking. *Nat Biotechnol* **2016**, *34* (8), 828–837. https://doi.org/10.1038/nbt.3597.
(21) Barrett, T.; Dowle, M.; Srinivasan, A.; Gorecki, J.; Chirico, M.; Hocking, T.; Schwendinger, B.; Krylov, I. Data.Table: Extension of `data.Frame`, 2006, 1.18.2.1. https://doi.org/10.32614/CRAN.package.data.table.
(22) Yang, S.; Sadilek, M.; Lidstrom, M. E. Streamlined Pentafluorophenylpropyl Column Liquid Chromatography–Tandem Quadrupole Mass Spectrometry and Global 13C-Labeled Internal Standards Improve Performance for Quantitative Metabolomics in Bacteria. *Journal of Chromatography A* **2010**, *1217* (47), 7401–7410. https://doi.org/10.1016/j.chroma.2010.09.055.
(23) Wakamatsu, A.; Morimoto, K.; Shimizu, M.; Kudoh, S. A Severe Peak Tailing of Phosphate Compounds Caused by Interaction with Stainless Steel Used for Liquid Chromatography

and Electrospray Mass Spectrometry. *J of Separation Science* **2005**, *28* (14), 1823–1830. https://doi.org/10.1002/jssc.200400027.

(24) New, L.-S.; Chan, E. C. Y. Evaluation of BEH C18, BEH HILIC, and HSS T3 (C18) Column Chemistries for the UPLC-MS-MS Analysis of Glutathione, Glutathione Disulfide, and Ophthalmic Acid in Mouse Liver and Human Plasma. *Journal of Chromatographic Science* **2008**, *46* (3), 209–214. https://doi.org/10.1093/chromsci/46.3.209.

(25) Ten-Doménech, I.; Martínez-Sena, T.; Moreno-Torres, M.; Sanjuan-Herráez, J. D.; Castell, J. V.; Parra-Llorca, A.; Vento, M.; Quintás, G.; Kuligowski, J. Comparing Targeted vs. Untargeted MS2 Data-Dependent Acquisition for Peak Annotation in LC–MS Metabolomics. *Metabolites* **2020**, *10* (4), 126. https://doi.org/10.3390/metabo10040126.

(26) Alseekh, S.; Aharoni, A.; Brotman, Y.; Contrepois, K.; D'Auria, J.; Ewald, J.; C. Ewald, J.; Fraser, P. D.; Giavalisco, P.; Hall, R. D.; Heinemann, M.; Link, H.; Luo, J.; Neumann, S.; Nielsen, J.; Perez De Souza, L.; Saito, K.; Sauer, U.; Schroeder, F. C.; Schuster, S.; Siuzdak, G.; Skirycz, A.; Sumner, L. W.; Snyder, M. P.; Tang, H.; Tohge, T.; Wang, Y.; Wen, W.; Wu, S.; Xu, G.; Zamboni, N.; Fernie, A. R. Mass Spectrometry-Based Metabolomics: A Guide for Annotation, Quantification and Best Reporting Practices. *Nat Methods* **2021**, *18* (7), 747–756. https://doi.org/10.1038/s41592-021-01197-1.

(27) Pičmanová, M.; Moses, T.; Cortada-Garcia, J.; Barrett, G.; Florance, H.; Pandor, S.; Burgess, K. Rapid HILIC-Z Ion Mobility Mass Spectrometry (RHIMMS) Method for Untargeted Metabolomics of Complex Biological Samples. *Metabolomics* **2022**, *18* (3), 16. https://doi.org/10.1007/s11306-022-01871-1.

(28) Correia, M. S. P.; Othman, A.; Zamboni, N. Fast, General-Purpose Metabolome Analysis by Mixed-Mode Liquid Chromatography–Mass Spectrometry. *Analyst* **2025**, *150* (22), 4955–4961. https://doi.org/10.1039/D5AN00641D.

Acknowledgements: We thank Els Meert for the preparation of metabolite standards. This work was supported by VIB-KU Leuven Center for Microbiology and FWO Odysseus Type II funding (Grant number G0AT025N)